Fast Calculation of 3D Conductive Target Backscatter in a Random Medium using Coherence Based Monte Carlo Integration (CBMI) Method

G. Togtema[1], H. El-Ocla[1,2], and M. Al Sharkawy[3]

[1] Lakehead University, Thunder Bay, ON, Canada
gtogtema@lakeheadu.ca, hosam@lakeheadu.ca

[2] University of Bahrain, Bahrain

[3] Department of Electronics and Communication Engineering, Arab Academy for Science, Technology & Maritime Transport, Alexandria, Egypt
msharkawy@aast.edu

Abstract – In this paper, a fast method to perform backscattering calculations from perfect electrically conducting (PEC) objects embedded in continuous random media is presented. The current generator method (CGM) is revisited and is modified for speed, removing the need to perform matrix inverse operations. The presented formulations are adequate to solve two and three dimensional problems. A Monte Carlo technique will be employed to speed the high ordered integration by using the de-correlation in space found within the fourth moment of Green's function as an 'importance sampling' distribution. This incoherence is explicitly shown in the current generator formulation. The revisited formulation has improved functionality in its ability to consider three dimensional objects. Its algorithmic performance is analyzed and is found to be significantly faster than other candidate matrix based methods.

Index Terms – Current generator method, electric field integral equation, monostatic backscatter, Monte Carlo integration, radar cross section, and random media.

I. INTRODUCTION

Prior knowledge of monostatic backscattering from particles and objects is a useful tool for radar and optical imaging instrumentation. It helps to classify the returned signal into target types like snow, light / dense rain, wind, etc. [1, 2]. Furthermore, it helps the aircraft developers to optimize the effectiveness of the plane body design in a way to hide from radar, preventing a costly guess-and-test prototyping process. Calculating the scattering profile from arbitrarily shaped conducting targets is becoming trivial as a research question since many methods already exist: physical optics (PO), method of moments (MoM), finite difference time domain (FDTD). To be accurate, this task is straight forward when one neglects the space between the target and the observer, opting to consider only 'free space' conditions. On the other hand, when the aircraft is surrounded by random media (i.e., clouds, air pressure fluctuations, fog, rain, snow etc.); the calculation becomes significantly slow and some of the above methods produce erroneous results due to various physical conditions.

In this paper, the current generator method [3, 4] is revisited and altered to remove any inverse matrix operations. The complexity of the quadruple surface integral found in the electric field integral equation (EFIE) by the MoM can be reduced by implementing the Monte Carlo integration as will be shown later. Sampling points on the target surface are chosen such that they are most likely to contribute to the integration, neglecting those that do not. This probability distribution is based on signal coherence properties. Thus, the modified current generator method outperforms the MoM in

Submitted On: May 9, 2013
Accepted On: Oct. 14, 2013

terms of its asymptotic complexity with respect to the number of basis functions, and the usage of the coherence Monte Carlo integration provides an even larger improvement in computation speed. It is well known that calculating the backscattered intensity of large targets requires a quadratic polynomial increase in sample points. Thus, computational time saving of this method may facilitate quick calculations of large targets like stealth aircrafts.

II. THE CURRENT GENERATOR METHOD

This approach is a boundary value method, and as such, we express the backscattered field as a function of current density on the boundary of the object. Due to the targets being PEC, either the Dirichlet condition (u(r) = 0) for E-wave incidence or the Neumann condition ($\frac{\partial u(r)}{\partial n}$= 0) holds on the surface, and will greatly simplify the final expressions. Since there is little difference in the current generator method between the two configurations, we develop the method for E-wave incidence for simplicity's sake and refer to the current generator in H waves so the reader can make an analogy [5].

We start by re-emphasizing the radar process: incident wave, $u_{in}(\mathrm{r}_1)$ is generated by a sou rce distribution, $f(\mathrm{r}_t)$, and travels in the random media. It is transformed on the target into current, which then acts as a new source to reradiate to the observer. Mathematically, and rather intuitively, u_s(r), is related to the E-wave polarized incident field via [6],

$$u_s(r) = \int_s \int_s G(r \mid r_2)[Y(r_2 \mid r_1) u_{in}(r_1)] dr_1 dr_2 \quad (1)$$

where $Y(r_2|r_1)$ is a current generator operator that maps incident field to target surface current density, r_1 is the wave incidence point and r_2 is the point at which current is generated due to $u_{in}(r_1)$. Here, G($r|r_2$) satisfies the following Helmholtz equation for random media. The entire spatial fluctuations are represented by dielectric variation [7],

$$\left[\nabla^2 + k_0^2 \left(1 + \delta\varepsilon(r)\right)\right] G(r \mid r_2) = \delta(r - r_2) \ . \quad (2)$$

Here, k_0 is the wave number in free space, and $\delta\varepsilon$(r) is the spatial fluctuation of dielectric. According to the current generator method [6, 8], we expand the surface current, $J_s(\mathrm{r}_2)$ into harmonics and find an expression for their coefficients,

$$J_s(r_2) = \sum_{m=0}^{M} \sum_{n=0}^{N} b_{mn} \Psi_{mn}(r_2) \ . \quad (3)$$

Here, $\Psi_{mn}(\mathrm{r}_2)$ is the three dimensional basis function and b_{mn} is its weighting coefficient. For a given coordinate system, this, albeit, places its limitations on the shapes of considerable targets. Nevertheless, for any target depicted by, say, spherical coordinates, the function

$$\Psi_{mn}(r) = sqrt(2/\pi) k_0 j_n(k_0 r) y_m^n(\theta, \phi) \quad (4)$$

solves the separable wave equation and therefore its set reconstructs any current distribution [9]. Here, $y_m^n(\theta, \emptyset) = \sqrt{\frac{2n+1}{4\pi} \frac{(n-m)!}{(n+m)!}} P_m^n(sin\emptyset) e^{im\theta}$ is the spherical harmonic function and P_m^n is the Legendre function of degree n and order m. More details on the choice of basis functions and its properties are given in the appendix, but it suffices to say Ψ_{mn}(r) in equation (4) forms an orthonormal set according to [10]. This orthogonality is used in the following approach to arrive at an expression for the coefficients, b_{mn}, much in the same way they are for the Fourier transform. We multiply equation (3) by $\Psi^*_{m'n'}(\mathrm{r}_2)$ on both sides and integrate over the target surface,

$$\int_s \Psi^*_{m'n'}(r_2) J_s(r_2) dr_2 = \sum_{m=0}^{M} \sum_{n=0}^{N} b_{mn} \int_s \Psi_{mn}(r_2) \Psi^*_{m'n'}(r_2) dr_2 \ . \quad (5)$$

The orthogonal property of Ψ_{mn}(r) states,

$$\int_s \Psi_{mn}(r_2) \Psi^*_{m'n'}(r_2) dr_2 = \delta_{m,m'} \delta_{n,n'} \quad (6)$$

where the definition of the delta function is,

$$\delta_{m,m'} = \begin{cases} 1 & m = m' \\ 0 & m \neq m' \end{cases} \quad (7)$$

which is similar for $\delta_{n,n'}$. The normal part of the orthonormal property of $\Psi_{mn}(\mathrm{r}_2)$ ensures that the value of $\delta_{m,m'}$ for $m = m'$ is indeed 1, a nd not a normalizing constant. With the orthogonal relationship, equation (5) reduces to an equation where m' and n' becomes a pa rticular value of m and n, respectively, and thus the summations are dropped. We are left with

$$b_{mn} = \int_s J_s(r')\Psi^*_{mn}(r')dr' \ , \tag{8}$$

where r' denotes an arbitrary integration parameter on *S*. In the following section, we derive another expression for J_s(r') which, when substituted into equation (8) provides a more useful expression for b_{mn}.

A. Expression for the surface current

According to Huygen's principle [11],

$$u_s(r) = \int_s \left[u(r_2)\frac{\partial G(r\,|\,r_2)}{\partial n_2} - G(r\,|\,r_2)\frac{\partial u(r_2)}{\partial n_2} \right] dr_2 \tag{9}$$

where n_2 is the unit normal from the target surface *S*. When the Dirichlet boundary condition is applied, this becomes

$$u_s(r) = -\int_s G(r\,|\,r_2)\frac{\partial u(r_2)}{\partial n_2} dr_2 \,. \tag{10}$$

This is analogous to equation (1) where $\int_s Y(r_2|r_1)u_{in}(r_1)dr_1 = J_s(r_2)$, yielding,

$$J_s(r_2) = -\frac{\partial u(r_2)}{\partial n_2} \,. \tag{11}$$

Finally, we use equation (11) to determine the current generator operator by applying to equation (8),

$$b_{mn} = -\int_s \frac{\partial u(r')}{\partial n'}\Psi^*_{mn}(r')dr' \,. \tag{12}$$

B. The current generator operator

Considering that the total field, the sum of incidence and scattering, is zero on the target (u(r') = u_{in}(r') + u_s(r') = 0), we can expand the expression of b_{mn} in equation (12) to add the extra terms,

$$\begin{aligned} b_{mn} = &-\int_s \begin{bmatrix} \Psi^*_{mn}(r')\dfrac{\partial u_{in}(r')}{\partial n'} \\ -u_{in}(r')\dfrac{\partial \Psi^*_{mn}(r')}{\partial n'} \end{bmatrix} dr' \\ &-\int_s \begin{bmatrix} \Psi^*_{mn}(r')\dfrac{\partial u_{s}(r')}{\partial n'} \\ -u_{s}(r')\dfrac{\partial \Psi^*_{mn}(r')}{\partial n'} \end{bmatrix} dr' \,. \end{aligned} \tag{13}$$

Applying the Divergence theorem and using the radiation condition as in [8, 11], we find

$$\int_s \Psi^*_{mn}(r')\frac{\partial u_s(r')}{\partial n'} - u_s(r')\frac{\partial \Psi^*_{mn}(r')}{\partial n'} = 0 \tag{14}$$

and hence,

$$b_{mn} = -\int_s \begin{bmatrix} \Psi^*_{mn}(r')\dfrac{\partial u_{in}(r')}{\partial n'} \\ -u_{in}(r')\dfrac{\partial \Psi^*_{mn}(r')}{\partial n'} \end{bmatrix} dr' \,. \tag{15}$$

With the expression of b_{mn}, we can now use equations (1), (3), and (15) to obtain the expression for the current generator.

$$\begin{aligned} Y(r_2\,|\,r_1)u_{in}(r_1)dr_1 = -\int_s \sum_{m=0}^{M}\sum_{n=0}^{N} \\ J_s(r_2) = -\int_s \Psi_{mn}(r_1)\left[\Psi^*_{mn}(r_1)\frac{\partial}{\partial n_1} - \frac{\partial \Psi^*_{mn}(r_1)}{\partial n_1} \right] \\ u_{in}(r_1)dr_1 \ . \end{aligned} \tag{16}$$

This equations is, by analogy, the current generator operator acting on u_{in},

$$\begin{aligned} \Psi_{mn}(r_2)\times \\ Y(r_2\,|\,r_1) = -\sum_{m=0}^{M}\sum_{n=0}^{N}\left[\Psi^*_{mn}(r_1)\frac{\partial}{\partial n_1} - \frac{\partial \Psi^*_{mn}(r_1)}{dn_1} \right]. \end{aligned} \tag{17}$$

We now have the expression for one term in equation (1). Note that, unlike previous current generator formulations [5, 6, 8], the expression for Y (r_2| r_1) does not require the computation of a matrix inverse. The inverse integral transform property found in equation (8) allows for this simplification. As we will see, however, equation (1) is a little less straight forward due to random media components, and needs revisiting. The following section completes the current generator formulation and establishes a basis for CBMI.

III. RADAR SIGNAL COHERENCE AND RANDOM MEDIA

Any signal is comprised of both coherent and incoherent parts,

$$u(r) = \langle u(r) \rangle + \Delta u(r) \tag{18}$$

where the ensemble average, $\langle u(r)\rangle$ denotes the coherent component at the observer while Δu represents the incoherent part. Based on equation (18), one can rewrite the scattered equations due to an E-wave polarized incident field,

$$u_s(r) = \int_s dr_1 \int_s dr_2\, Y(r_2|r_1)G(r_1|r_t)G(r|r_2) \tag{19}$$

$$\langle u_s(r)\rangle = \int_s dr_1 \int_s dr_2\, Y(r_2|r_1)\langle G(r_1|r_t)G(r|r_2)\rangle. \tag{20}$$

Here, the $u_i(r_1)$is displayed in its Green's function representation. Fundamentally, $u_i(r_1) = \int_{V_T} G(r_1|r')f(r')dr'$, where r'describes the source distribution. For a source of unit strength, the $u_i(r_1)$ has been replaced with its point source Green's function representation, $u_i(r_1) \cong G(r_1|r_t)$, where $r_t$is the position of the transmitter within V_T. For monostatic conditions, $r_t = r$, so $u_i \cong G(r|r_1)$ after reciprocity has been employed $G(r_1|r) = G(r|r_1)$. Since radar antennas measure signal power, and not field, one must take the average of u_s^2 as,

$$\langle|u_s(r)|^2\rangle = \int_s d^4r\, Y(r_2|r_1)Y^*(r'_2|r'_1) \times \langle G(r|r_1)G(r|r_2)G^*(r|r'_1)G^*(r|r'_2)\rangle \tag{21}$$

where r_1 is the point of incidence, $r_2$is the point where the current is generated due to $u_i(r_1)$, r_1' and r_2' are the indices for complex waves of incidence and scattering, respectively, finally, $\int_s d^4r = \int_s dr_1 \int_s dr_2 \int_s dr'_1 \int_s dr'_2$. This expression is still too analytically complex. In addition to evaluating the product of the current generator, the average of the Green's function needs to be simplified.

A. Fourth moment of Green's function in random media

The fourth moment of Green's function, M_2, in equation (21) is simplified using a common statistical identity,

$$\langle UV\rangle = \langle U\rangle\langle V\rangle + covariance(U,V) \tag{22}$$

leading to,

$$M_2 \cong \langle G(r|r_1)G^*(r|r'_1)\rangle\langle G(r|r_2)G^*(r|r'_2)\rangle + \langle G(r|r_1)G^*(r|r'_2)\rangle\langle G(r|r_2)G^*(r|r'_1)\rangle. \tag{23}$$

In order for this to be true, the incidence wave must sufficiently uncorrelated from the scattered wave [12]. Many natural processes, like those in the atmosphere, are aggregations of independent and identically distributed variables that have Gaussian distribution. To be even more complete, one can consider a small region of free space around the target to minimize the likelihood of reflected waves passing through the same random media as during incidence [6, 7]. We can view the fourth moment decomposition approximation as just that, something with sources of error, and therefore do not require this extra region. To describe the problem as to be practically accepted, however, restrictions on the random media intensity, $B = \langle\delta\varepsilon(r)\delta\varepsilon(r')\rangle \ll 1$, and scale size, $l \gg 1$ must be kept to remove the depolarization effects. The first term in equation (23) represents the low spatial frequencies in the media (*lf*), while the second term is the base for high spatial frequency (*hf*) expansion. Furthermore, judging from research into the spatial frequency spectrum of atmospheric air flow velocity structure function [13], its wave number $k_{\delta\varepsilon}$ decays proportional to a strong negative power ~ $k_{\delta\varepsilon}^{-5/3}$. This indicates there is little natural high frequency energy as far as air pressure is concerned that would invalidate the above approximation. One could place a low-pass filter on their random media spectrum without much detriment to accuracy.

B. Second moment of Green's function

The two expressions M_2^{lf} and M_2^{hf} are the products of the 2nd moment of Green's function M_1. The expression of M_1 in random media is expressed as,

$$M_1 = M_1^i m(\rho_0 d) \tag{24}$$

$$M_1^i = G_0(r|r_1)G_0(r|r_2), \tag{25}$$

$$m(\rho_0 d) = exp\left\{-\frac{k_0}{4}\int_{z_0}^{z} D_t\left[\frac{z'-z_0}{z-z_0}(\rho_0 d), z'|z_0\right]dz'\right\}, \tag{26}$$

$$D_t[\rho, z'|z_0] = \int_0^{z-z_0} D\left[\rho, z-\frac{z'}{2}, z'\right]dz', \tag{27}$$

$$D\left[\rho, z-\frac{z'}{2}, z'\right] = 2\begin{bmatrix} B\left(0, z-\frac{z'}{2}, z'\right) \\ -B\left(\rho, z-\frac{z'}{2}, z'\right)\end{bmatrix}. \tag{28}$$

Here, G_0 is the Green's function in free space, and D is the random medium structure function in the transverse plane [14]. The symbol ρ is the

transverse distance from the primary axis (i.e., the line of sight) and $\rho_{0d} = \rho_2 - \rho_1$. The symbol z is the coordinate along the primary axis of the observer and z_0 describes the target size. Further description on the problem configuration is illustrated in Fig. (1).

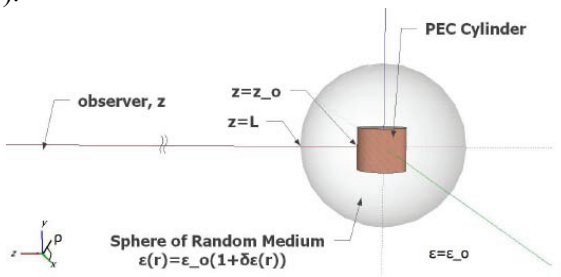

Fig. 1. Problem description of a 3D PEC target in random medium.

C. Expression of the coherent backscattered intensity

The expression of the backscattered power for a conductive target in random media is calculated through the product of the current generators and the derived expression of M_2, which can be shown as,

$$\langle |u_s(r)|^2 \rangle = \int_s d^4 r_{(1,2,1',2')} \times \left[\sum_{m=0}^{M} \sum_{n=0}^{N} \Psi_{mn}(r_2) \frac{\partial X}{\partial n_2} \left\{ \Psi_{mn}^*(r_1) \frac{\partial X}{\partial n_1} - \frac{\partial \Psi_{mn}^*(r_1)}{\partial n_1} \right\} \right] \times \left[\sum_{m=0}^{M} \sum_{n=0}^{N} \Psi_{mn}^*(r_2') \frac{\partial X}{\partial n_2'} \left\{ \Psi_{mn}(r_1') \frac{\partial X}{\partial n_1'} - \frac{\partial \Psi_{mn}(r_1')}{\partial n_1'} \right\} \right] \times (M_\alpha + M_\beta) M_0. \quad (29)$$

where,

$$M_\alpha = exp\left\{ -\frac{k_0^2}{4} \mu\gamma(z, z_0) [(\rho_1 - \rho_1')^2 + (\rho_2 - \rho_2')^2] \right\}, \quad (30)$$

$$M_\beta = exp\left\{ -\frac{k_0^2}{4} \mu\gamma(z, z_0) [(\rho_2 - \rho_1')^2 + (\rho_1 - \rho_2')^2] \right\}, \quad (31)$$

$$M_0 = \frac{1}{[8\pi k_0 (z - z_0)]^2} exp(X), \ \mu = \sqrt{\pi} \frac{BL^3}{l(z - z_0)^2}, \quad (32)$$

and

$$X = -jk_0 \left(z_1 - z_1' + z_2 - z_2' \right) + \frac{j k_0}{2(z - z_0)} \left(\rho_1^2 - \rho_1^{2'} + \rho_2^2 - \rho_2^{2'} \right). \quad (33)$$

IV. COHERENCE BASED MONTE CARLO INTEGRATION

The quadruple surface integral found in equation (29) makes computations very slow and memory intensive. A mesh grid of even ten samples in each of the θ and ϕ directions discretizes the target into 100 samples, making the four-fold integration require $100^4 = 10^8$ evaluations of the integrand. Each of M_0, M_α and M_β may also have 10^8 allocations in memory. Due to the oscillatory nature of the basis functions, Ψ_{mn}, the exponential decay of M_α and M_β, and the target dependent nature of $\frac{\partial X}{\partial n}$, it is logical to think that certain points on the mesh will not contribute to the integration. Avoiding computational efforts toward these "useless" points is the reason why Monte Carlo integration is used. Consequently, the integrand is evaluated at a random set of sample points that have a probabilistic emphasis toward converging to the true answer faster. An estimate of the mean value of the integrand is calculated and from the Mean Value Theorem the integral is determined. Mathematically, denoting the integrand of equation (29) as I, the integral

$$\left\langle \left| u_s(r) \right|^2 \right\rangle = \int_s d^4 r . I \quad (34)$$

that can be calculated by the expected value of the integrand via

$$\langle I \rangle = \frac{1}{A^4} \int_s d^4 r . I \qquad \int_s d^4 r . I = A^4 \langle I \rangle, \quad (35)$$

where A is the surface area of the target. Introducing a normalized function, R, leads,

$$\left\langle \left| u_s(r) \right|^2 \right\rangle = \int_s d^4 r . \frac{I(r_{1,2,3,4})}{R(r_{1,2,3,4})} R(r_{1,2,3,4}) = \int_s \frac{I(r_{1,2,3,4})}{R(r_{1,2,3,4})} d\hat{R}(r_{1,2,3,4}) \quad (36)$$

where $r_{1,2,3,4}$ are the four integral dependence and $\hat{R}(r_{1,2,3,4}) = \int_0^{r_{1,2,3,4}} R(r'_{1,2,3,4}) d r'_{1,2,3,4}$. Here, the zero vector, 0, denotes any starting point for the surface

integration, and $r'_{1,2,3,4}$ is an arbitrary parameter on S. Making the change of variables, $t = R(r)$ rewrites equation (34) as

$$\left\langle \left| u_s(r) \right|^2 \right\rangle = \int_{\hat{R}(r)} \frac{I\left(\hat{R}^{-1}(t)\right)}{R\left(\hat{R}^{-1}(t)\right)} dt . \tag{37}$$

The difference between equation (34) and equation (37) is that, in the former, a uniform sampling distribution within $r_{1,2,3,4}$ may produce elements of $I(r_{1,2,3,4})$ that do not effectively contribute to $\langle I \rangle$, where as the latter does if I/R deviates less from the mean than I alone. At run time, one can check the variance of the estimate via,

$$\mathrm{var}\left(\langle I \rangle\right) = \frac{\left\langle \left(\frac{I}{R}\right)^2 \right\rangle - \left\langle \frac{I}{R} \right\rangle^2}{N_r} \tag{38}$$

where N_r is the number of samples already calculated at run time. The whole idea lies in the choice of the sampling points.

A. Interpreting coherent backscattered intensity

The Monte Carlo method described above has an effective I/R arrangement when the function, R, 'follows' the integrand; when the distribution is zero or large, so should the integrand. Paradoxically, we are unable to generate the perfect distribution since we would need to know the analytic expression of equation (29) and hence not need Monte Carlo integration in the first place. Therefore we look at the expression in equation (29) and break down its physical meaning to provide insight on the choice of R.

The interpretation is very similar to that of other work, namely the combined field integral equation (CFIE) in [15], but with an added term for random media. The expression for M_0 is the complex free space propagation 'transfer function' between the source field intensity and the received field intensity. It represents the effect of the $1/r$ power law while taking into account spatial sinusoidal changes due to $e^{jk_0 r}$. The expressions for M_α and M_β each have $exp\{-\mu\gamma\rho^2 D\}$ dependence (where ρD is used to denote the difference between the appropriate ρ's for either M_α or M_β), which can be explained as the signal decorrelation due to the random media effects μ and γ. Lastly, the expression within the square brackets, as mentioned in [15], is the translation response from incident wave to current density. We denote this as a unit plane wave response of current. To see this, the total field intensity integral equation (not just the coherent intensity) has a fourth moment of $M_2 = M_0$, and not $M_2 = M_0$ ($M_\alpha + M_\beta$) [5]. M_0 is already exposed as the propagation transfer function, and the square brackets is the only remaining physical process: the generation of current on the target. To summarize,

$$U_{TF} = M_0 \tag{39}$$

$$U_{dec} = M_\alpha + M_\beta \ , \tag{40}$$

$$U_p = \left[\sum_m^M \sum_n^N \left\{ \Psi_{mn}(r_2) \frac{\partial X}{\partial n_2} \times \left(\Psi^*_{mn}(r_1) \frac{\partial X}{\partial n_1} - \frac{\partial \Psi^*_{mn}(r_1)}{\partial n_1} \right) \right\} \right] \times \left[\sum_m^M \sum_n^N \left\{ \Psi^*_{mn}(r_2') \frac{\partial X}{\partial n_2'} \times \left(\Psi_{mn}(r_1') \frac{\partial X}{\partial n_1'} - \frac{\partial \Psi_{mn}(r_1')}{\partial n_1'} \right) \right\} \right], \tag{41}$$

where the subscripts TF means propagation transfer function, dec means a de correlating function, and p is for the plane wave response.

B. Choice of 'importance sampling' distribution

For an observer positioned very far from the target, U_{TF} does not vary much from one point on the target to the next. Therefore, our easiest choice for R closely resembles the uniform distribution and does not follow the integrand well. The next easiest choice comes from U_p. It is somewhat easy to emulate since it has a common factor within the summation,

$$U_p = \left(NM \frac{\partial X}{\partial n_2} \right) \left(NM \frac{\partial X}{\partial n_2'} \right) \times \left[\sum_m^M \sum_n^N \left\{ \Psi_{mn}(r_2) \times \left(\Psi^*_{mn}(r_1) \frac{\partial X}{\partial n_1} - \frac{\partial \Psi^*_{mn}(r_1)}{\partial n_1} \right) \right\} \right] \times \left[\sum_m^M \sum_n^N \left\{ \Psi^*_{mn}(r_2') \times \left(\Psi_{mn}(r_1') \frac{\partial X}{\partial n_1'} - \frac{\partial \Psi_{mn}(r_1')}{\partial n_1'} \right) \right\} \right], \tag{42}$$

where $\frac{\partial X}{\partial n}$ can be found under the far field approximation $(z-z_0) >> 1$ as,

$$\frac{\partial X}{\partial n_1} = \hat{n}_1 \cdot \nabla X = \hat{n}_1 \cdot \pm jk_0 \begin{pmatrix} \hat{z} + \frac{4\rho_1 x_1}{2(z-z_0)}\hat{x} \\ + \frac{4\rho_1 y_1}{2(z-z_0)}\hat{y} \end{pmatrix} \quad (43)$$
$$\simeq jk_0 \hat{n}_1 \cdot \hat{z}_1 .$$

Unfortunatly, choosing $R = jk_0\left(\hat{n}_1 \cdot \hat{z}_1 - \hat{n}_1' \cdot \hat{z}_1'\right)$ will only speed up i ntegration in the r_1 and r_1' directions. Furthermore, if the target boundary is not analytic, we will need to perform surface integral computations to normalize R via

$$\int_s dr_1 \int_s dr_1' R = 1, \quad (44)$$

rendering the algorithm slow. Lastly, the most powerful choice of R lies in U_{dec}. Due to the sharp descent of the $exp\{-\mu\gamma\rho^2 D\}$ function, the signal contribution from different sections on t he target that would normally occur in free space may no longer be correlated (coherent). This effect is excellent to consider as a sampling distribution to emphasize the presence of random media. The choice of

$$R = \frac{M_\alpha\left(r_{1,2,1',2'}\right) + M_\beta\left(r_{1,2,1',2'}\right)}{\int d^4 r_{1,2,1',2'}\left[M_\alpha\left(r_{1,2,1',2'}\right) + M_\beta\left(r_{1,2,1',2'}\right)\right]}, \quad (45)$$

samples points that are most likely to be coherent and hence the name coherence based Monte Carlo integration (CBMI) is the most appropriate.

V. COMPUTATIONAL INTENSITY

In this section, the current generator and the CBMI are analyzed for their computational performance. These advantages are compared to that of the MoM.

A. Generation of basis coefficients

CBMI and the current generator's performance relative to the MoM technique depend on the management of basis vectors. MoM performances are specified as it applies to manipulating the bases vectors, often assuming an analytic fourth moment in free space that does not slow the computation process. Considering different Green's functions (like that in random media) will add extra complexity on account of the integration. A traditional MoM approach involves filling the $N_b \times N_b$ coefficient matrix whose elements represent interdependence of bases (inner products), storing this information in memory, and solving the linear system. Here, N_b is the number of unknown basis functions. According to [16] and [17], this approach has a computational complexity of $\mathbf{O}(N_b^2)$ for each step. Assuming a double summation expression, which one would expect for the term I of the current generator method shown in equation (34), where the summation inside the integrand computes very simple terms. This in turn, causes the current generator to have a very fast effective "fill time" of $\mathbf{O}(N_b)$, where a matrix is not needed. Fast Fourier Transform method (FFT) has matrix filling and solving complexities of $\mathbf{O}(N_b^{1.5} \log N_b)$ and Adaptive Cross Approximation (ACA) algorithms scale to $\mathbf{O}(N_b^{4/3} \log N_b)$ for moderately sized targets [18]. Fast Multipole Method (FMM) and multilevel FMM (MLFMM), which have achieved $\mathbf{O}(N_b \log N_b)$ in free space, are dependent on the analytical form of Green's function and can be translated to account for random media [16]. Ultimately, neither of these achieve the ultimate goal of removing interdependence among bases to reduce the complexity from $\mathbf{O}(N_b^2)$ to $\mathbf{O}(N_b)$.

B. CBMI computational intensity

The quadruple integral required by the current generator equation should scale with a complexity of $\mathbf{O}(N_s^4)$, if one were to use a quadrature integration. However, as the number of sample points increases in CBMI, the estimate of the Monte Carlo integral decreases and, according to the law of large numbers, its variance reduces as $1/\sqrt{N_s}$. This continues until an acceptable error level has been reached. Therefore, the quadruple surface integral within the current generator method that requires N_s^4 points using quadrature integration should converge as $\sqrt{N_s^4} = N_s^2$ using CBMI. As previously noticed, the double summation over M and N adds an extra order of complexity, bringing the overall performance of equation (34) to $\mathbf{O}(N_s^3)$. This is better than the MoM, that brings the its total complexity to $\mathbf{O}(N_s^{5.5})$.

VI. ALGORITHM PERFORMANCE

While asymptotic analysis is useful, especially when assessing targets of large electrical size, it is important to consider computational advantages. The first is how Monte Carlo implementation stops once it has achieved a low variance in its estimate. One can make this stopping threshold fairly high since calculations need not be more precise than the noise floor of the receiver system. To be specific, $\mathrm{var}\left(A^4\langle I\rangle\right) < k_bT \cdot R_a \cdot \Delta v \cdot G \cdot F^2$ where k_bT is the thermal energy, Δv is the bandwidth of the receiver, R_a is the antenna resistance, G is the antenna sensitivity to electric field, and $F = noise_{out} \,/\, Gain \cdot noise_{in}$ is the voltage noise figure of the preamp. In Radar Systems, one can choose a noise floor of a predetermined strength (e.g. ~ -60 *dBm*) and use G to determine the level of var($A^4\langle I\rangle$). Due to the Gaussian-Like nature of the integrand of equation (34), there is a confident feel that var($A^4\langle I\rangle$) represents more accurately the error. A second speed advantage is that knowledge of the system at hand can reduce the algorithm speed. Knowing the number of wavelengths on the target determines the number of harmonic modes required. Moreover, CBMI lends itself to be used easily in parallel processing applications. Due to the integral being evaluated as an average of sample points, tasks can be distributed among many modules, each performing their own estimate of $\langle I\rangle$, with almost no modification to the algorithm.

VII. CONCLUSION

We have presented a method for the fast calculation of backscatter from arbitrary 3D PEC objects embedded in continuous random media for E-wave polarization. The method was developed for 3D targets in spherical coordinates but could be applied to targets that conform to any other system (cylindrical, polar etc.). The formulation of a field intensity integral equation called the current generator method was modified to not contain any matrix inverse operations. This expression was broken into physical processes and a Monte Carlo integration based on the signal decorrelation greatly reduced the total algorithmic computational complexity to $\mathbf{O}(N_s^3)$ compared to that of fast MoM ($\sim\mathbf{O}(N_s^{5.5})$). Signal decorrelation, as described by M_α and M_β, depends heavily on the second moment of Green's function, whose analytical expression is described and is very involved. The consideration of random media characteristics, intensity and distribution are, therefore, critical aspects in adapting the formulation to specific scenarios. The computational speed shows promise and may justify the efforts. Since, by the Nyquist criterion, N_s is tied directly to $(k_0a)^2$, backscattered intensity calculations of airplanes observed by UHF and higher frequencies may become possible with the decrease in complexity.

ACKNOWLEDGMENT

This work was supported in part by the National Science and Engineering Research Council of Canada (NSERC) under Grant 250299-02.

REFERENCES

[1] T. Otto and H. Russchenberg, "Estimation of specific differential phase and differential backscatter phase from polarimetric weather radar measurements of rain," *IEEE Geosci. Remote Sens. Letters*, vol. 8, no. 5, pp. 988-992, 2011.

[2] J. Leinonen, D. Moisseev, V. Chandrasekar, and J. Koskinen, "Mapping radar reflectivity values of snowfall between frequency bands," *IEEE Trans. Geosci. Remote Sens.*, vol. 49, no. 8, pp. 3047-3058, 2011.

[3] S. Chang, C. Fleuraru, Y. Mao, and S. Sherif, "Attenuation compensation for optical coherence tomography imaging," *Optics Commun.*, vol. 282, pp. 4530-4507, 2009.

[4] H. El-Ocla and M. Tateiba, "Strong backscattering enhancement for partially convex targets in random media," *Waves Rand. Media*, vol. 11, pp. 21-32, 2001.

[5] H. El-Ocla, "Effect of the illumination region of targets on waves scattering in random media with H-polarization," *Waves Rand. Complex Media*, vol. 19, no. 4, pp. 637-653, 2009.

[6] H. El-Ocla, "Target configuration effect on wave scattering in random media with horizontal polarization," *Waves Rand. Complex Media*, vol. 19, no. 2, pp. 305-320, 2009.

[7] Z.-W. Xu, J. Wu, Z.-S. Wu, and L.-W. Li, "Analytical solution to the n-nth moment equation of wave propagation in continuous random media," *IEEE Trans. Antennas and Prop*., vol. 55, no. 5, pp. 1407-1415, 2007.

[8] M. Tateiba and Z. Meng, "Wave scattering from conducting bodies embedded in random media-

theory and numerical results," *Prog. Electromag. Research*, vol. 14, pp. 317-361, 1996.

[9] A. Ishimaru, *Electromagnetic Wave Propagation, Radiation, and Scattering*, pp. 112-114, 1991.

[10] Q. Wang, O. Ronneberger, and H. Burkhardt, "Fourier analysis in polar and spherical coordiantes," *Published Internal Report* http://lmb.informatik.unifreiburg.de/papers, 2008.

[11] A. Ishimaru, *Electromagnetic Wave Propagation, Radiation, and Scattering*, pp. 149-153, 1991.

[12] R. Frehlich and M. Kavaya, "Coherent laser radar performance for general atmospheric refractive turbulence," *Applied Optics*, vol. 30, no. 36, pp. 5325-5352, 1991.

[13] E. Lindborg, "Can the atmospheric kinetic energy spectrum be explained by two-dimensional turbulence?," *J. Fluid Mech.*, vol. 388, pp. 259-288, 1999.

[14] A. Ishimaru, *Wave Propagation and Scattering in Random Media*, pp. 512, 1997.

[15] L. Zhanhe, H. Peilin, G. Xu, L. Ying, and J. Jinzu, "Multi-frequency RCS reduction characteristics of shape stealth with MLFMA with improved MMN," *Chinese J. Aeronautics*, vol. 23, pp. 327-333, 2010.

[16] R. Burkholder and J.-F. Lee, "Fast dual-MGS block-factorization algorithm for dense MoM matrices," *IEEE Trans. Antennas Prop.*, vol. 52, no. 7, pp. 1693-1699, 2004.

[17] P. De Vita, F. De Vita, A. Freni, P. Pirinoli, F. Vipiana, and G. Vecchi, "Performances of MR-preconditioned fast MoM techniques," *Microwave Opt. Tech. Letters*, vol. 52, no. 8, pp. 1719-1724, 2010.

[14] K. Zhao, M. Vouvakis, and J.-F. Lee, "The adaptive cross approximation algorithm for accelerated method of moments computations of EMC problems," *IEEE Trans. EMC*, vol. 47, no. 4, pp. 763-773, 2005.